Modeling and Control of SMT Manufacturing Lines Using Hybrid Dynamic Systems[†]

L.G. Barajas[1], A. Kansal[2], A. Saxena[2], M. Egerstedt[1], A. Goldstein[1], and E.W. Kamen[1]

[1] Georgia Institute of Technology, Electrical and Computer Engineering,
Center for Board Assembly Research
Atlanta, GA 30332, USA
{lbarajas,magnus,alex.goldstein,ed.kamen}@ece.gatech.edu
http://www.cbar.marc.gatech.edu
[2] Georgia Institute of Technology, Textile and Fibre Engineering
Atlanta, GA 30332, USA
{gtg982b,gtg989b}@mail.gatech.edu

Abstract. In this paper we show how hybrid control and modeling techniques can be put to work for solving a problem of industrial relevance in Surface Mount Technology (SMT) manufacturing. In particular, by closing the loop over the stencil printing process, we obtain a robust system that can recover from faulty initial settings, adapt to environmental changes and unscheduled interrupts, and remove discrepancies associated with bidirectional printing machines. Moreover, a timed Petri net argument is invoked for bounding the control effort in such a way that the throughput of the system is unaffected by the introduction of the closed-loop controller. The soundness of the approach is verified on a real SMT manufacturing line.

1 Introduction

To close the loop around the Stencil Printing Process (SPP) in Surface Mount Technology (SMT) manufacturing has long been a desirable yet evasive goal in the industry [2, 7, 12, 15, 14]. By closing the loop it is envisioned that the system will recover from faulty initial settings, adapt to environmental changes and unscheduled interrupts, and remove discrepancies associated with bidirectional printing machines. However, the reason why this problem is particularly challenging is threefold. First, as of yet, no detailed process models have been derived [7, 12, 14], which implies that traditional, model-based control algorithms are of limited use. Secondly, the high noise levels in the process, combined with aggressive temporal variations in performance due to environmental factors such as humidity and temperature, make data-driven models unsuitable as a basis for

control. Thirdly, due to the prohibitive cost (both temporal and monetary) associated with printing a large number of boards, sufficient excitation is a luxury that can not be afforded, i.e. system identification techniques can not be applied.

In this paper we report on our findings when designing a closed-loop control algorithm that overcomes all of these difficulties by switching between different modes of operation as the performance of the process changes. In particular, a coarse search algorithm is used for driving the system to a desired operating band, at which point a statistical, least-squares based controller is introduced for managing the mean and variance of the process. However, additional constraints are put on the controller that can be derived from a higher-level process management point of view. It is vitally important that the introduction of a closed-loop control module does not affect the throughput of the process. Furthermore, by printing boards concurrently the control value obtained when inspecting board k will not necessarily affect board $k+1$. Instead a careful trade-off between delay times, throughput, and control performance must be made, for which a timed Petri net model of the process will be used.
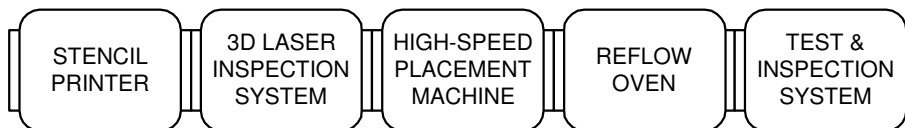
The contribution of this paper can thus be thought of as the development of hybrid process models at both the process management and the process dynamics levels, as well as a solution to an industrially relevant control problem in SMT manufacturing, and the outline of this paper is as follows: In Sect.2 a description of the SPP is given in some detail and in particular the performance objectives and process constraints are presented, followed by a Petri net based analysis of the system in Sect.3. In Sect.4 the hybrid control algorithm is given, and the experimental results are presented in Sect.5.

2   Stencil Printing

The goal of the SPP in SMT manufacturing of Printed Circuit Boards (PCB) is to apply an accurate and repeatable volume of solder paste deposits at precise locations [8, 10, 18]. It has been shown that a majority of the defects in the final boards can be attributed to the SPP [2, 14, 16], which makes this step the most critical in the process. Therefore, any attempt to enhance the performance of the line should start with the SPP. Furthermore, a defect that occurs in the early stages of the process will propagate, causing reworking over-costs at each additional step in the process that the PCB goes through without being detected as defective. This stresses the importance of early detection not only of obvious printing errors (e.g., extreme lack or excess of solder paste in a solder brick), but also of possible causes of other defects resulting from degradation of solder paste quality, loss of the working viscosity point, or even machine-related failures.

A simplified version of the SMT manufacturing process is illustrated in Fig.1. In order to solder components to a PCB, it is necessary to "print" solder paste bricks over the metallic contact pads on the board. Once this is successfully achieved and verified by optical or laser inspection, the components are placed on top of the solder bricks and their leads are pushed into the solder paste. When the components have been attached, the solder paste is melted using

either reflow soldering or vapor-phase soldering to create the electro-mechanical junctures. Finally, the manufactured PCBs are inspected and tested.

| STENCIL PRINTER | 3D LASER INSPECTION SYSTEM | HIGH-SPEED PLACEMENT MACHINE | REFLOW OVEN | TEST & INSPECTION SYSTEM |

Fig. 1. SMT manufacturing line

The SPP is illustrated in Fig.2. In the first phase, a metallic stencil is placed over the PCB and solder paste is kneaded on one side of the stencil. During the second phase, the squeegee is pushed over the stencil and is moved from one side to the other of the stencil with a speed and pressure that can be set by the operator. (This squeegee speed is furthermore the control parameter that we adjust in our proposed closed-loop control algorithm.) This procedure makes the solder paste roll to fill the apertures in the stencil. In the final phase, before components, such as BGAs, QFPs, and, 0201s are placed over the solder bricks, a squeegee blade is used for removing excess material from the stencil, and then separate the stencil from the PCB.

The performance of the SPP can heuristically be characterized by how well the solder bricks are being printed. The objective of a closed-loop control law is thus to adapt the machine settings in such a way that the solder bricks satisfy certain regularity conditions. The industry standard for measuring the quality characteristics of the process is solder-paste-volume deposition [3, 11, 6, 9]. Commonly, a direct sample mean of such values is used as quality characteristics, while a more elaborated approach would be to assign different weights to each solder brick type so that problematic components can be given more importance in the quality characteristics generation process. Such a weighted scheme can be represented by a weighted sample mean

$$\overline{H}_W(n) = \sum_{i=1}^{Q} w_i h(n,i), \quad \sum_{i=1}^{Q} w_i = 1, \quad w_i \geq 0, \tag{1}$$

where Q is the number of solder bricks present in the nth board, $h(n,i)$ is the height of the ith solder brick, and w_i is the weight assigned to that particular brick.

The SPP depicted in Fig.2 is a high-noise process corrupted by two types of noise: measurement inaccuracies and internal system variability. The former can normally be disregarded when 3-D laser measurement techniques are used, while the latter has a six-sigma interval of approximately $\pm 30\%$ of the mean of the probability distribution function of the signal [3], making the process outputs highly variable even under constant conditions. (A typical output histogram of
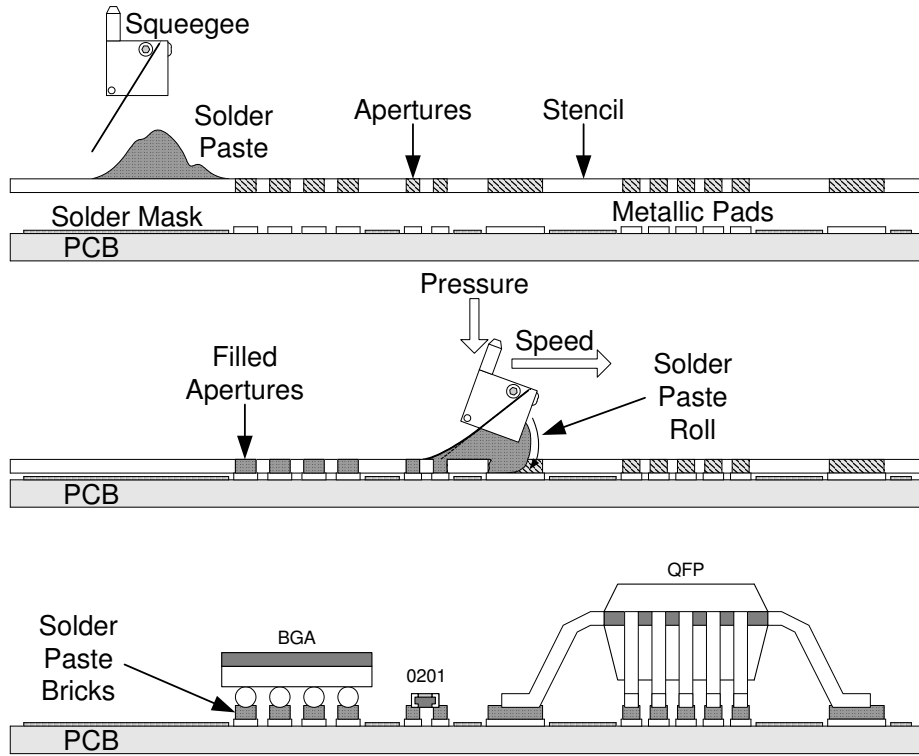
Fig. 2. Stencil printing process

the process can be seen in Fig.8(a).) We can thus assume that the process is given by $y = F(C) + v$, where C is the control action corresponding to the squeegee speed and y is the weighted sample mean of the brick height. Furthermore, F is an unknown function of the control variable C, and v is the process noise.

Now, given some value H_d for the desired brick height, the objective is to determine an appropriate squeegee speed C_d such that $||F(C_d) - H_d||$ is suitably small. In particular, what we want to achieve is to reach a desirable process performance while printing as few boards as possible, i.e. using few measurements. Secondly, for the SPP, no dynamical models are as of yet available due to the highly complex process dynamics [7, 12, 14] and we need to bound the control variability in order to suppress the transient effects associated with changing the control value. The third constraint that we impose is that we want the control law to rapidly reach a desired operating point and then remain close to that point for all future control values. If F is known this problem can be solved using dynamic programming (see for example [4]), but for the problem under consideration in this paper, no such assumptions can be made. Hence only suboptimal solutions can be obtained.

The suboptimal yet effective solution proposed in Sect.4 consists of a hybrid control law that satisfies the constraints, while achieving fast convergence. However, before we can start investigating the details of this control law, some words about higher-level issues must be made. In particular, it must be decided how much computation time is available to the control module without affecting the throughput of the system, which can be done based on a timed Petri net model of the SPP.
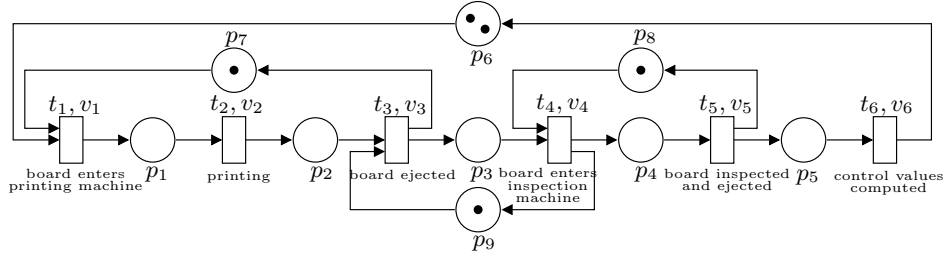
3 Timed Petri Net Models

In order to analyze the temporal behavior of the SPP, a timed Petri net model of the stencil printing machine, the inspection machine, and the control module is depicted in Fig.3, where transitions t_1, t_2, t_3 define the operation of the stencil printer, where solder paste is deposited on the board. The inspection machine, in which the measurement of the quality of the solder bricks is conducted, is given by transitions t_4 and t_5. The place p_3 is the buffer in between the two machines, and $M_0(p_9)$ corresponds to the capacity of the buffer. (This capacity is 1 in Fig.3, but it is in fact one of the parameters that should be chosen when designing a control strategy.) Transition t_6 corresponds to the computation of control values, and $M_0(p_6)$ indicates the "board-delay" imposed by the control law. The interpretation is as follows: If $M_0(p_6) = 1$ then the control value obtained from board k directly affects board $k+1$, i.e. no boards are being printed until a control value has been computed. However, the stencil printer is in fact operating in two decoupled directions, i.e. board k is printed with the squeegee blade moving forward, while board $k + 1$ is printed in a backwards direction.

Due to the discrepancies in performance in the two printing directions shown in Fig.8(a), where Dir 0 and Dir 1 denote forward and backward directions respectively, we will assume that $M_0(p_6) = 2c, \ c = 1, 2, \ldots$, or in other words, that the control values computed from boards printed in the forward direction only affects other boards printed in that direction and vice versa for backwards boards. What we want to do in this section is thus to compute the throughput and cycle time of the Petri net, and then design the intermediary buffer size $M_0(p_9)$ and controller look-back $c = M_0(p_6)/2$ in such a way that the control delay is as small as possible.

3.1 Timing and Buffer Size Considerations

The model in Fig.3 is a so-called *marked graph* [17], i.e. the weights are all equal to one and each place in the Petri net has a unique input and output transition. For such marked graphs, the following equations describe the temporal behavior of the Petri net:

$$\begin{cases} \pi_{i,k+M_0(p_i)} = \tau_{r,k}, \quad \text{where } {}^\circ p_i = \{t_r\} \\[2ex] \tau_{j,k} = \max\left\{\tau_{j,k-1}, \max_{p_i \in {}^\circ t_j}\{\pi_{i,k}\}\right\} + v_{j,k}, \end{cases} \tag{2}$$

Fig. 3. Timed Petri net model for the SPP with online controller.

where $\pi_{i,k}$ denotes the time at which place p_i receives its kth token, $M_0(p_i)$ is the initial marking of p_i, $°p_i$ denotes the set containing the unique input transition to p_i. Furthermore, $\tau_{j,k}$ denotes the time at which transition t_j fires its kth time, $°t_j$ denotes the set of input places to t_j, and $v_{j,k}$ defines the delay-time between t_j becoming fireable for the kth time and its firing.

We first note that the inspection machine is the bottle-neck machine in the SPP, i.e. that $v_1 + v_2 + v_3 < v_4 + v_5$. We do not want the introduction of a control law to slow down the process, i.e. reduce the throughput, so an initial assumption is that

$$v_1 + v_2 + v_3 + v_6 < v_4 + v_5. \tag{3}$$

In order to simplify the computations we furthermore assume initially that $M_0(p_9) = \infty$, i.e. that the buffer capacity is infinite, which corresponds to removing the loop containing p_9 in Fig.3. Under this assumption the timing equations give that $\tau_{5,k} = \tau_{5,k-1} + v_4 + v_5$, when k is large enough to suppress the effects caused by the initial markings. What this means is that the throughput, ρ, of the system is $\rho = 1/(v_4+v_5)$, i.e. that the cycle time of the PN is $CT_{PN} = 2c(v_4+v_5)$, since a total number of $2c = M_0(p_6)$ tokens are cycling through the PN. An additional relevant measure is the process cycle time, i.e. the time that a board spends in the SPP, which is given by $CT = CT_{PN} - v_6$, since the $(k + 2c)^{th}$ control evaluation takes place after the kth board has left the SPP.

Under the infinite buffer capacity assumption and the assumption that $v_4 + v_5 > v_1 + v_2 + v_3 + v_6$, an accumulation of printed boards occurs in the buffer p_3. It furthermore follows that $M(p_3) \in \{2c-2, 2c-1\}$, i.e. that the actual number of tokens in the buffer changes between $2c - 2$ and $2c - 1$ for durations T_1 and $v_5 + v_4 - T_1$ respectively, where T_1 can be computed as follows:

$$\begin{aligned} T_1 &= \tau_{3,2c-1+k} - \tau_{4,k} = \tau_{1,2c-1+k} + v_2 + v_3 - \tau_{4,k} \\ &= \pi_{6,k-1+M_0(p_6)} + v_1 + v_2 + v_3 - \tau_{4,k} \\ &= \tau_{6,k-1} + v_1 + v_2 + v_3 - \tau_{4,k}. \end{aligned} \tag{4}$$

But, since t_4 and t_6 become fireable simultaneously, i.e. $\tau_{6,k-1} - v_6 = \tau_{4,k} - v_4$, we get $T_1 = v_1 + v_2 + v_3 + v_6 - v_4$, and the following relation holds:

$$M(p_3) = \begin{cases} 2c - 2 & \text{for a duration of } v_1 + v_2 + v_3 + v_6 - v_4 \\ 2c - 1 & \text{for a duration of } v_5 + 2v_4 - v_1 - v_2 - v_3 - v_6. \end{cases} \tag{5}$$

If we now assume that the buffer capacity is finite then it is clear that the case when $M_0(p_9) \geq 2c - 1$ is identical to the case when $M_0(p_9) = \infty$ due to the fact that no more than $2c - 1$ boards are present in the buffer at any given time. However, when $M_0(p_9) < 2c - 1$, the process dynamics change in the following manner: The inspection time is now long enough for the accumulation of the boards to occur at p_3, while the accumulation is restricted by the bound on the capacity of the buffer. Thus the place p_6 will always contain $2c - M_0(P_9) - 2$ tokens, since two tokens are in the inspection and printing machine. We would expect the buffer to be full after transients, i.e. that $M(p_3) = M_0(p_9)$. But, there are instances of duration v_3 when $M(p_3)$ drops to $M_0(p_9) - 1$. This happens when the buffer p_3 is full and t_3 is waiting for a token in p_9. As soon as t_4 fires, p_3 looses one token but t_3 becomes fireable.

Hence, for any value of controller look-back c, we get the number of boards in the buffer p_3 after transients as

$$M(p_3) = \begin{cases} M_0(p_9) - 1 & \text{for a duration of } v_3 \\ M_0(p_9) & \text{for a duration of } v_4 + v_5 - v_3. \end{cases} \tag{6}$$

The inspection machine is still the bottleneck machine, which implies that the throughput of the PN remains the same. But the SPP cycle time becomes $CT = (M_0(p_9) + 1)(v_4 + v_5) + v_5 - v_3$, since the printed board has to wait inside the printing machine before ejecting as the buffer p_3 is full.

3.2 Discussion

The controller look-back c directly affects the process performance. The response time increases with increasing c as the process control values for the nth board are computed based on the inspection data of the $(n - c)^{th}$ board printed in the same direction. But the process performance also depends on the time available to compute the process control values, i.e. on v_6. As the available computation time increases, more complex statistical computations can be carried out in order to achieve higher accuracy. Since the throughput is limited by the inspection time, we can decrease the waiting time of the boards in p_3 and make this time available for computation instead, without affecting throughput. Thus, if we increase v_6 (assuming that $v_1 + v_2 + v_3 \leq v_4 + v_5$, i.e. printing takes less time than inspection), then the maximum value to which v_6 can be increased ($\hat{v}_6$) without affecting the throughput can be found as follows:
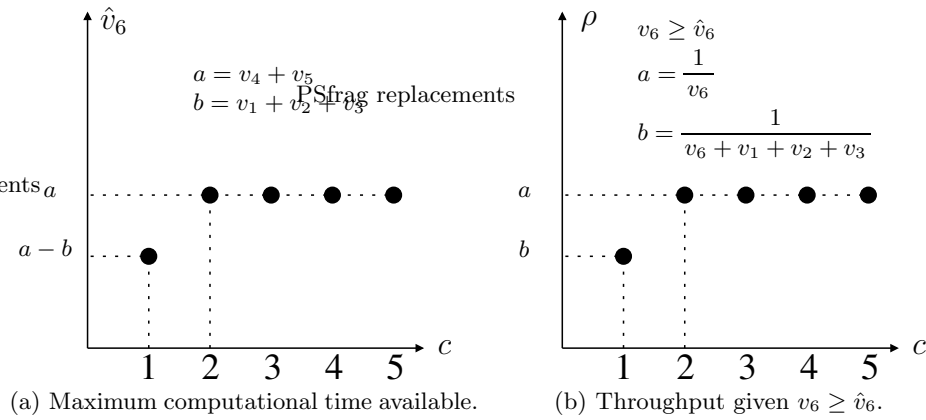
If we increase computation time s.t. $v_6 > v_4 + v_5$, then $M(p_5)$ increases due to accumulation of tokens in p_5 and once the effect of transients is suppressed, $M(p_5) \in \{2c - 2, 2c - 1\}$. The time taken to suppress the transients depends on the magnitude of v_6 and the controller look-back c. This accumulation in p_5 leads

8   L.G. Barajas et al.

to idling of the inspection machine causing a decrease in the throughput. Thus, $\hat{v}_6 = v_4 + v_5$. But, if the controller look-back is one, the control value of the kth inspected board should be generated and the $(k+2)^{th}$ board should be printed before the inspection of the $(k+1)^{th}$ board completes, meaning that $\tau_{6,k}$, $\tau_{1,k+2}$, $\tau_{2,k+2}$ and $\tau_{3,k+2}$ should occur before $\tau_{5,k+1}$, i.e. before the inspection machine goes idle. Thus, we obtain the maximum time available to compute the control values as shown in Fig.4(a) and calculated as

$$\hat{v}_6 = \begin{cases} v_4 + v_5 - (v_1 + v_2 + v_3) & \text{if } c = 1 \\ v_4 + v_5 & \text{if } c > 1. \end{cases} \tag{7}$$

An interesting point to note here is that, until $v_6 \leq \hat{v}_6$, inspection time is the bottleneck and governs the throughput of the system. But once v_6 increases beyond $\hat{v}_6$, computation becomes the bottleneck, i.e. the throughput of the system is reduced. The throughput ρ, for $v_6 \geq \hat{v}_6$, and as a function of the controller look-back is depicted in Fig.4(b) and is given by

$$\rho = \begin{cases} \frac{1}{v_6 + v_1 + v_2 + v_3} & \text{if } c = 1 \\ \frac{1}{v_6} & \text{if } c > 1. \end{cases} \tag{8}$$

(a) Maximum computational time available.   (b) Throughput given $v_6 \geq \hat{v}_6$.

Fig. 4. In the left figure, the maximum available computation time $\hat{v}_6$ is depicted as a function of the controller look-back. The right figure shows the relationship between the throughput ρ and the controller look-back.

To summarize: The performance of the process depends on the controller look-back c and the available computation time v_6. A small c ensures lower response time whereas larger v_6 provides more time for computations, generating better control values, which can improve the process quality and efficiency. Thus, ideally we should keep the controller look-back as small as possible, i.e. let c be

equal to one, and have $v_6 = \hat{v}_6$. However, if $c = 1$, the response time improves but $\hat{v}_6$ decreases by $v_1 + v_2 + v_3$. This tradeoff can be decided on the basis of the relative magnitudes of the v_i values. For instance, if the inspection time is significantly larger than the printing time ($v_4 + v_5 \gg v_1 + v_2 + v_3$) then one can expect that sufficient time to compute good control values is available. As a consequence, the controller look-back should be kept equal to one.

For the SMT manufacturing line at the Center for Board Assembly Research (CBAR) at the Georgia Institute of Technology, the v_i-values are of the order of $v_1 = 8\text{s}; v_2 = 20\text{s}; v_3 = 2\text{s}; v_4 = 2\text{s}; v_5 = 180\text{s}$. Thus, if we keep $c = 1$, the computation time available is

$$v_6 = (v_4 + v_5) - (v_1 + v_2 + v_3) = 150\text{s}. \tag{9}$$

On the other hand, the control law proposed in Sect.4 requires 15s to compute the control values with a 1GHz Intel Pentium III processor using Matlab compiled code. It may seem unnecessary to go through all these calculations to find out that the available time for computation is one order of magnitude larger than the current computation time of the algorithm. However, new technology in post-printing inspection machines is reducing v_5 below 60s in which case, v_6 will be heavily limited by the inspection time v_5. Also, the inspection time can be considerably reduced by performing partial inspection of only a percentage of the boards. This practice will be required when new technologies in placement machines make it necessary to reduce the cycle time for the SPP. Thence, for this machine, the controller look-back should be one. Also, for $c = 1$, the buffer between the printing machine never holds more than one board ($2c - 1$) so we can keep its capacity equal to one. This is what will be done for the remainder of this paper when we go on and actually construct the control module.

4   Hybrid, Data-Driven Control

The purpose of this section is to report on the control design, corresponding to transition t_6 in Fig.3. As pointed out in Sect.2, no explicit process model is available when designing the control law. Instead it can be noted that as long as the initial control value separations are large enough to recover the local sign of the slope of F, i.e. $\|F(C_0 + \Delta) - F(C_0)\| \geq 2a$, where C_0 is the initial squeegee speed, Δ is the step length, and the noise is assumed to take on values over $[-a, a]$, we recover a conjugated gradient direction. By using a fixed step length descent along the recovered direction, a locally optimal (over the quantized set of control values $\{C \in \Re \mid C = C_0 + k\Delta, \ k \in \mathbb{Z}\}$) control value can be obtained in a fixed number of steps, i.e. while printing few boards, as shown in [1]. Under additional assumptions about the unimodality of F, a globally optimal control value can furthermore be obtained over the quantized set.

Once the conjugated gradient search has terminated, a statistical fine-tuning of the squeegee speed (over $\Re$) can be used. We choose to work with a windowed version of a least-squares affine estimator of F, which can then be directly used to compute the control values.

In other words, given the static input-output map $y = F(C) + v$, we want to find an affine estimate of F as $F(C) = \theta_0 + \theta_1 C$ using the last N output values. With a slight abuse of notation we denote these by $y_1, \ldots, y_N$ and let $C_1, \ldots, C_N$ denote the corresponding N last inputs. What this implies is that N defines the size of the sample window. Thence, in order to recover the affine estimator parameters $\theta = [\theta_0 \ \theta_1]^{\mathrm{T}}$, the standard basis, given by the N×2-matrix M, can be formed from the unitary N-vector $b = [1 \ 1 \ \ldots \ 1]^{\mathrm{T}}$ and the control values vector $\mathbf{C} = [C_1 \ C_2 \ \ldots \ C_N]^{\mathrm{T}}$, arranged side by side such that $M = \begin{bmatrix} b \vdots \mathbf{C} \end{bmatrix}$.

Now, the classic LS solution [13] to the over-determined problem, $M\theta = \mathbf{y}$, where $\mathbf{y} = [y_1 \ y_2 \ \ldots \ y_N]^{\mathrm{T}}$, was shown in [3] to satisfy the following equation

$$\theta = \frac{\mathbf{C}^{\mathrm{T}} \left[\left(\frac{\mathbf{C}b^{\mathrm{T}} - \mathbf{C}^{\mathrm{T}}b\mathbb{I}_N}{N\mathbb{I}_N - bb^{\mathrm{T}}} \right) \otimes \mathbf{y} \right]}{\mathbf{C}^{\mathrm{T}}(N\mathbb{I}_N - bb^{\mathrm{T}})\mathbf{C}} \quad , \tag{10}$$

where $\mathbb{I}_N$ is the $N \times N$ identity matrix. Equation (10) can thus be used to calculate the parameters θ of the affine estimator, and for the sake of clarity, it should be noticed that

$$\left(\frac{\mathbf{C}b^{\mathrm{T}} - \mathbf{C}^{\mathrm{T}}b\mathbb{I}_N}{N\mathbb{I}_N - bb^{\mathrm{T}}} \right)$$

is a partition matrix which operates (using the Kronecker product ($\otimes$)) on the vector $\mathbf{y}$ of data samples. An extensive explanation of the complete controller can be found in [3], and the switched control law that we propose in this paper is thus given by two distinct stages:

1. A constrained conjugated-gradient search for reaching the desired operational band is used in the first part of the control law.
2. A least-squares affine estimator for maintaining and fine-tuning the process constitutes the second part.

The switched control strategy is depicted in Fig.5 as a directed graph, or hybrid automaton, and the interpretation of the process dynamics, transition guards, and resets are as follows: The two main states are q_{GS} and q_{LS} corresponding to the gradient-search and least-squares parts respectively. A transition from the machine idling (q_{STOP}) to q_{GS} occurs when the external control variable u_{EXT} is equal to $START$, at which point the squeegee speed is set to C_0. (We used $C_0 = 0.5$in/sec in the experiments in Sect.5). Once the locally optimal control value $C^\star$ is obtained, a transition occurs to the least-squares part of the algorithm, at which point a reset initializes the least-squares parameters θ. If the performance of the least-squares algorithm deteriorates, a new gradient search is conducted. However, if the performance is too poor ($\|y_d - y\| > W$), for some error bound W, then this is an indication that the stencil needs to be manually wiped. The last state of the hybrid automaton (q_{PAUSE}) is entered if the process cycle time, CT, as defined in the previous section, exceeds 5min. If, after the pause state is entered, the process is restarted within 20min, no gradient search is needed, while $CT \in [20, 45]$min indicates that a new search is needed. These additional states are required in order to capture the complex nature of
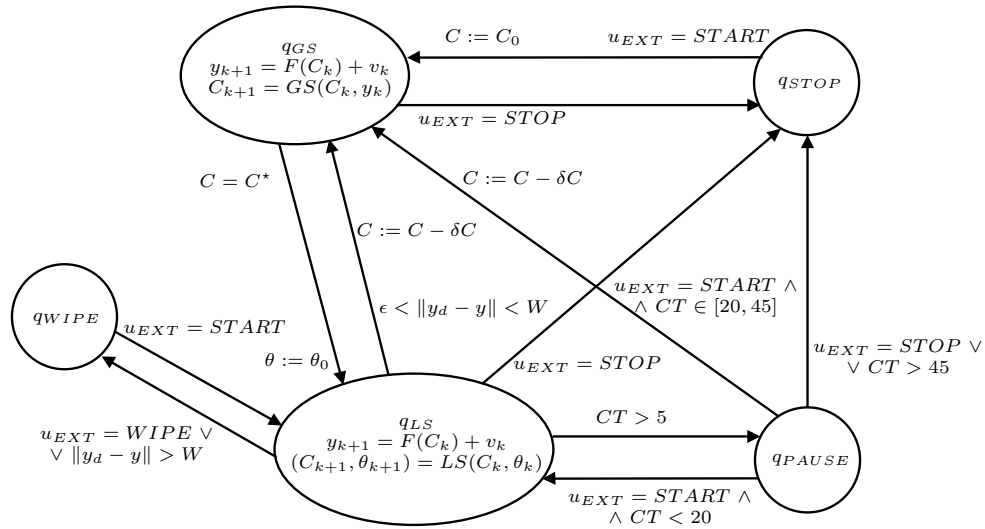
Fig. 5. Stencil printing process hybrid automaton.

the process, and in order to be able to adapt to external events affecting the process. The most important one of them being the pause of the production line due to a external input. Depending on the duration of the disturbance, the process should be recovered, restarted or stopped in order to maintain or restore the printing quality.

The choice of the guards based on the temporal variable CT is critical for the correct operation of the hybrid automaton. The guards have been empirically chosen using the parameters and materials stated in Sect.5. For very a low viscosity solder paste, these values should be reduced from the order of minutes to only seconds such that the working viscosity point of the solder paste can be effectively recovered.

According to the taxonomy proposed in [5] the hybrid automaton in Fig.5 can be characterized as follows:

- *Autonomous Switchings*: The *cycle time CT* triggers transitions in this category. The CT-variable is synchronized with a continuous time clock but is reset every time a new board is printed.
- *Autonomous Impulses*: This type of behavior is always present in the SPP because a bidirectional printing technique is used. As a direct consequence of this, it is necessary to switch between two controllers after each board is printed. Each of these controllers operates in either forward or backward directions. The differences in printing direction can account up to for a 10% difference in the mean height of the solder bricks of any given board.
- *Controlled Switchings*: This is the normal operation modality of the controller while it is in the *affine least-squares* estimator mode q_{LS}. The external input

$u_{EXT} \in \{START, STOP, WIPE\}$ can be classified as having this kind of structure.
− *Controlled Impulses*: This is the standard operation modality of the controller while in the *gradient search* mode q_{GS}.

In the following section we will illustrate the usefulness of the proposed switched control strategy by applying it to the SPP at the CBAR SMT manufacturing line.

5   Experimental Results

The hybrid control algorithm proposed in this paper is used for generating control values for the stencil printing process. The input control variable is squeegee speed and the output is the weighted sample mean of the height of the deposited solder bricks. A 12in metallic blade at a constant pressure setting of 12lb/in^2 was used to perform the procedure over a laser-cut 5mil (127μm) stencil, using non-clean 63/37 (tin/lead%) solder paste Type IV.

The experimental setup used for this paper includes a Speedline MPM-3000 stencil printer and a CyberOptics Sentry-2000 3D-Laser inspection system which are part of one of the Surface Mount Technology (SMT) manufacturing lines at the Center for Board Assembly Research (CBAR) at the Georgia Institute of Technology.

Figure 6 shows the control values as the hybrid algorithm goes through the different operational modes. Additionally, the case when a large disturbance is introduced is considered. In this case, the output setting is changed by -25% after the 13th iteration, and Fig.7 shows how the algorithm is able to adapt to this sudden set-point change in only a few iterations.

Figure 8 shows the effect of the controller over the process in a real production run. This plot demonstrates how the controller discriminates between printing directions and by adjusting the weighted sample mean on a board-by-board basis independently in each direction it aligns the solder brick height distributions to the desired mean height. Depicted are the output histograms generated with and without the controller. It should be noted that the distribution in Fig.8(b) is center around the desired target height H_d of 5.5mil (139.7μm). As marked for reference in Fig.8, the stencil thickness S_t in the experiment under consideration is 5mil (127μm).

6   Conclusions

In this paper we show how hybrid control and modeling techniques can be put to work for solving a problem of industrial relevance in SMT manufacturing by closing the loop over the stencil printing process. A timed Petri net argument is invoked for bounding the control effort in such a way that the throughput of the system is unaffected by the introduction of the closed-loop controller. The actual control law is comprised of a switched algorithm that, in stage one,
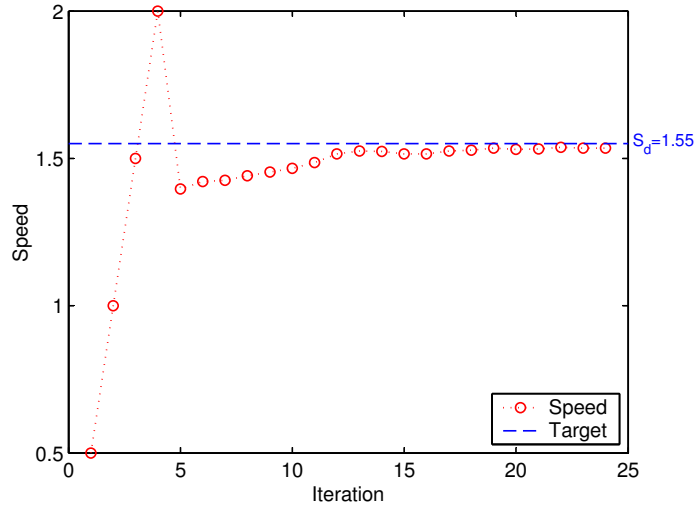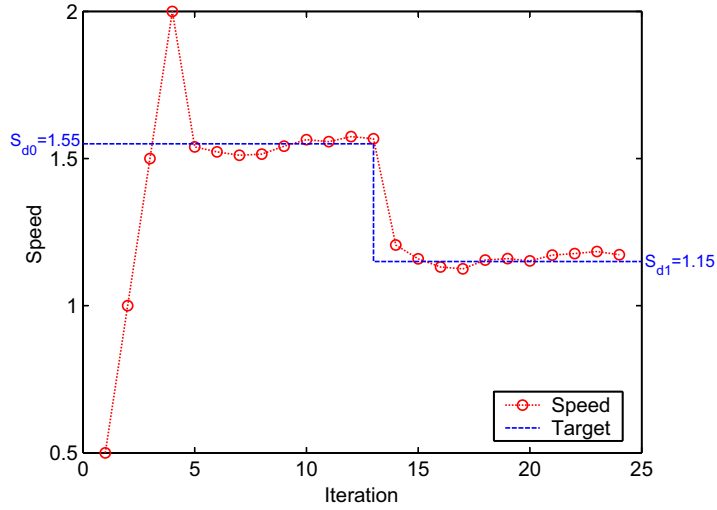
Fig. 6. Constant desired height.

Fig. 7. Step applied to desired height.

quickly reaches a desirable band of operation using a constrained, conjugated gradient search. In stage two, a windowed version of a least squares algorithm is applied to shape the distributions of the solder brick heights around the desired brick height, and the soundness of the approach is verified on a real SMT manufacturing line.

(a) Without closed-loop control.   (b) With closed-loop control.
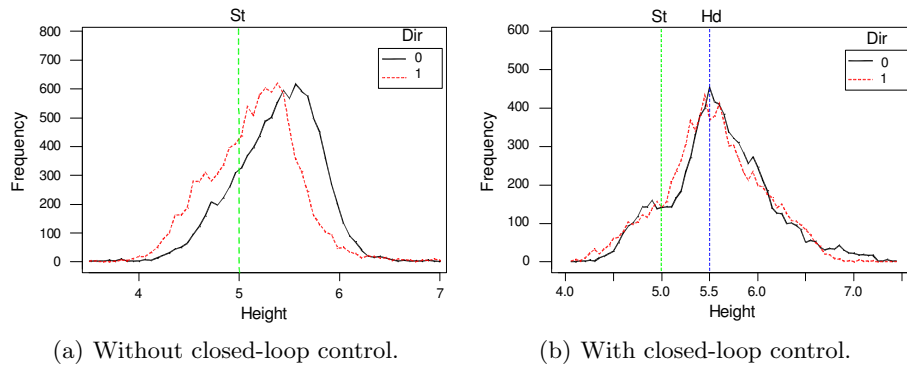
Fig. 8. Process histograms.

References

1. Barajas, L.G., Egerstedt, M., Kamen, E.W., Goldstein, A.: Process control in a high-noise environment with limited number of measurements. To appear in: *2003 American Control Conference*, Denver, CO (2003)
2. Barajas, L.G., Kamen, E.W., Goldstein, A.: On-line enhancement of the stencil printing process. *Circuits Assembly* (2001) 32–36
3. Barajas, L.G., Kamen, E.W., Goldstein, A., Egerstedt, M., Small, B.: A closed-loop hybrid control algorithm for stencil printing. In: *Surface Mount Technology Association International Conference (SMTA02)*, Boston, MA (2002) 51–58
4. Bertsekas, D.P.: *Dynamic programming and optimal control.* Athena Scientific (1995)
5. Branicky, M., Borkar, V., Mitter, S.: A unified framework for hybrid control: model and optimal control theory. *IEEE Transactions on Automatic Control*, **43** (1998) 31–45
6. Burr, D.: Solder paste inspection: process control for defect reduction. In: *Test Conference, 1997. Proceedings., International*, CyberOpt. Corp., USA (1997) 1036
7. Durairaj, R., Nguty, T.A., Ekere, N.N.: Critical factors affecting paste flow during the stencil printing of solder paste. *Soldering & Surface Mount Technology* **13** (2001) 30 – 34
8. Fujiuchi, S.: Fundamental study on solder paste for fine pitch soldering. In: *Electronics Manufacturing Technology Symposium, 1991., Eleventh IEEE/CHMT International*, IBM Japan, Shiga, Japan (1991) 163–165
9. Gopalakrishnan, L.: Continuous improvement of the solder paste deposition process through designed experiments. *IPC/SMTA Electronics Assembly Expo. Proceedings of the Technical Program* (1998)
10. Gopalakrishnan, L., Srihari, K.: Solder paste deposition through high speed stencil printing for a contract assembly environment. *Journal of Electronics Manufacturing* **8** (1998) 89–101
11. Husman, M.S., Rukavina, J.P., Yuan, G.: A study of solder paste volumes for screen printing. *Proceedings of the Technical Program. NEPCON West'93* (1993)
12. Johnson, A., Flori, A.: High density/fine feature solder paste printing. In: *Proceedings of APEX.* (2001)

13. Kamen, E.W., Su, J.: *Introduction to optimal estimation.* Advanced textbooks in control and signal processing. Springer, London ; New York (1999)
14. Lau, F.K.H., Yeung, V.W.S.: A hierarchical evaluation of the solder paste printing process. *Journal of Materials Processing Technology* **69** (1997) 79–89
15. Lotfi, A., Howarth, M.: *An intelligent closed-loop control of solder paste stencil printing stage of surface mount technology.* Nottingham Trent University. Department of Mechanical and Manufacturing Engineering, Nottingham (1998)
16. Pan, J., Tonkay, G., Storer, R., Sallade, R., Leandri, D.: Critical variables of solder paste stencil printing for micro-BGA and fine pitch QFP. In: *Electronics Manufacturing Technology Symposium, 1999. Twenty-Fourth IEEE/CPMT*, Dept. of Ind. & Manuf. Syst. Eng., Lehigh Univ., Bethlehem, PA, USA (1999) 94–101
17. Proth, J.M., Xie, X.: *Petri nets : a tool for design and management of manufacturing systems.* Wiley, New York (1996)
18. Venkateswaran, S., Srihari, K., Adriance, J., Westby, G.: A realtime process control system for solder paste stencil printing. In: *Electronics Manufacturing Technology Symposium, 1997., Twenty-First IEEE/CPMT International*, Dept. of Syst. Sci. & Ind. Eng., State Univ. of New York, Binghamton, NY, USA (1997) 62–67